Arab. J. Math. (2022) 11:49–66
https://doi.org/10.1007/s40065-022-00364-2
Arabian Journal of Mathematics

Sardor Tojiev

Boson stars with negative Gauss–Bonnet coupling

Received: 10 January 2022 / Accepted: 1 February 2022 / Published online: 16 February 2022

Abstract In this paper, we discuss asymptotically flat and anti-de Sitter (AdS) boson star in (4+1)-dimensional Gauss–Bonnet gravity. We describe the dependence of the mass, the charge and the radius of the boson star on the model parameters, such as Gauss–Bonnet coupling α, cosmological constant Λ and gravitational constant κ. The basic properties of the solutions of boson stars have been studied for the different negative values of Gauss–Bonnet coupling. We found that when κ is large and α is negative enough, the spiral shrinks and pulls back to the larger internal frequency ω, and there is only one branch exists. We have also observed that when κ is small enough and if α is close to zero, the spiral will unfold.

Mathematics Subject Classification (2000) 34B15 · 83C05 · 83D05 · 83E50

1 Introduction

In relativistic field theory, there are basically two types of solitons. They are called topological and non-topological solitons. Here we will consider the non-topological one which is called boson stars when coupled to gravity. Boson stars arise in field theories with unbroken continuous symmetry. They carry a non-vanishing Noether charge that is globally conserved. These solitons are localized, stable and regular solutions of the nonlinear field equations. The study of boson stars in higher dimensions in Anti-de Sitter (AdS) space-time has been considered by many authors in recent years [13,18,28,29]. One of the main motivations of the analysis of Einstein's equations with scalar field coupled to gravity in the presence of negative cosmological constant may shed new light on generic properties of particle-like solutions in asymptotically AdS space-time. On the other hand, the study of theories gravity coupled with scalar field attracted much interest by the discovery of Higgs boson which was announced by the ATLAS and CMS collaborations in July 2012 [6]. This discovery confirms the conjecture put forward in the 1960's and proves the existence of scalar field in nature.

Another example of non-topological solitons are Q-balls and they also have been discussed extensively by many authors [17,19]. Supersymmetric Q-balls and boson stars have been studied in [25,26]. Boson stars can be constructed making Q-balls self-gravitating. Within the Standard model the supersymmetric Q-balls have been considered as possible candidates for baryonic dark matter [23,32,33]. The detectability and gravitational redshift for boson stars with a self-interaction was discussed in [34]. There have been also a lot of investigations concerned with soliton and black hole solutions in AdS in Einstein–Gauss–Bonnet gravity [7–10,12,14] and in pure Einstein gravity [11,15,16,21,22,24].

S. Tojiev (✉)
Institute of Physics, University of Oldenburg, 26111 Oldenburg, Germany
E-mail: sardor@astrin.uz

S. Tojiev
Ulugh Beg Astronomical Institute, Astronomy Str. 33, 100052 Tashkent, Uzbekistan

In this paper, we study the Gauss–Bonnet boson stars in asymptotically flat and AdS space–time. We construct the solutions numerically using COLSYS [3,4] (Fortran ODE solver package). We describe the dependence of the mass M, charge Q and radius R of the boson stars on the model parameters such as the Gauss–Bonnet coupling α, the cosmological constant Λ and the gravitational constant κ. Previously, this subject has been studied in flat space-time in [28], but for positive α. Here we pay our attention to the negative case of this coupling parameter and also extended it studying in AdS space-time.

The paper is organized as follows: in Sect. 2, we introduce the basic model for boson star and derive the field equations using appropriate boundary conditions. Next, in Sect. 3, we present and discuss our numerical results for different values of model parameters. And finally, in Sect. 4, some concluding remarks are given.

Throughout the paper, we use a space-like signature as $(-, +, +, +)$ and a system of units $c = 1$.

2 The model

In this section we construct asymptotically flat and anti-de Sitter (AdS) boson stars in (4 + 1)-dimensional Gauss–Bonnet gravity. We consider standard Einstein–Gauss–Bonnet theory minimally coupled to a complex valued and self-interacting scalar field. The action for boson star model in five-dimensional anti-de Sitter space-time in Gauss–Bonnet gravity reads:

$$S = \int d^5x\sqrt{-g}(R - 2\Lambda + \alpha(R^{MNKL}R_{MNKL} - 4R^{MN}R_{MN} + R^2) + 16\pi G_5\mathcal{L}_{\text{matter}}), \tag{1}$$

where $\Lambda = -6/\ell^2$ is the cosmological constant, α is the Gauss–Bonnet coupling and G_5 is Newton's constant in 5 dimensions. $\mathcal{L}_{\text{matter}}$ is the matter Lagrangian for the complex scalar field ψ and reads :

$$\mathcal{L}_{\text{matter}} = -(\partial_\mu\psi)^*(\partial^\mu\psi) - U(\psi), \tag{2}$$

where $U(\psi)$ is the scalar field potential that arises in gauge-mediated supersymmetric breaking in the Minimal Supersymmetric extension of the Standard Model (MSSM) and it is given by the expression

$$U(\psi) = \begin{cases} m^2|\psi|^2 & \text{if } |\psi| \le \sigma \\ m^2\sigma^2 = \text{const.} & \text{if } |\psi| > \sigma, \end{cases} \tag{3}$$

where σ corresponds to the scale below which super-symmetry is broken, while m denotes the scalar boson mass. This potential is not differentiable at $|\psi| = \sigma$. Therefore the following approximation of the above potential has been suggested [20]:

$$U(\psi) = m^2\sigma^2\left(1 - \exp\left(-\frac{|\psi|^2}{\sigma^2}\right)\right). \tag{4}$$

For simplicity we develop this potential into a series and keep the terms only up to 6th order in ψ

$$U(\psi) = m^2|\psi|^2 - \frac{m^2|\psi|^4}{2\sigma^2} + \frac{m^2|\psi|^6}{6\sigma^4} + O\left(|\psi|^8\right). \tag{5}$$

Using the variation principle we can derive the gravity and Klein–Gordon equations as follows:

$$G_{MN} + \frac{\alpha}{2}H_{MN} = 8\pi G_5 T_{MN}, \tag{6}$$

$$\left(\Box - \frac{\partial U}{\partial|\psi|^2}\right)\psi = 0, \tag{7}$$

where the tensor H_{MN} is given by

$$\begin{aligned} H_{MN} = {} & 2\left(R_{MABC}R_N^{ABC} - 2R_{MANB}R^{AB} - 2R_{MA}R_N^A + RR_{MN}\right) \\ & -\frac{1}{2}g_{MN}\left(R^2 - 4R_{AB}R^{AB} + R_{ABCD}R^{ABCD}\right), \quad M, N, A, B, C = 0, 1, 2, 3, 4, \end{aligned} \tag{8}$$

and T_{MN} is the energy–momentum tensor

$$
\begin{aligned}
T_{MN} &= g_{MN}\mathcal{L} - 2\frac{\partial \mathcal{L}}{\partial g^{MN}} \\
&= -g_{MN}\left[\frac{1}{2}g^{KL}\left(\partial_K\psi^*\partial_L\psi + \partial_L\psi^*\partial_K\psi\right) + U(\psi)\right] + \partial_M\psi^*\partial_N\psi + \partial_N\psi^*\partial_M\psi. \qquad (9)
\end{aligned}
$$

Since the matter Lagrangian is invariant under the global U(1) transformation the system posses the locally conserved Noether current j^M and the globally conserved Noether charge Q. The symmetry for this transformation is given by

$$\psi \rightarrow \psi e^{i\chi}, \qquad (10)$$

with a conserved current:

$$j^M = -\frac{i}{2}\left(\psi^*\partial^M\psi - \psi\partial^M\psi^*\right), \qquad (11)$$

and a conserved charge, namely, the number of scalar particles:

$$Q = \int d^4x\sqrt{-g}\, j^0. \qquad (12)$$

2.1 Ansatz, field equations and boundary conditions

We choose the following Ansatz for the metric:

$$ds^2 = -NA^2dt^2 + \frac{1}{N}dr^2 + r^2\left(d\theta^2 + \sin^2\theta d\varphi^2 + \sin^2\theta\sin^2\varphi d\chi^2\right), \qquad (13)$$

where N and A are functions of r only. We further choose

$$N(r) = 1 - \frac{2n(r)}{r^2} - \frac{\Lambda}{6}r^2, \qquad (14)$$

such that $n(\infty)$ will determine the gravitational mass of the solution at infinity. For the scalar field, we choose the following stationary Ansatz

$$\psi(r,t) = \phi(r)e^{i\omega t}, \qquad (15)$$

where ω is the internal frequency and ϕ is function of r only.

Imposing the Ansatz (13) and (15) into the field equations (6), (7) we can derive the equations of motion as follows:

$$A'(r) = \frac{2\kappa r^3\left(A^2N^2\phi'^2 + \omega^2\phi^2\right)}{3AN^2\left(r^2 + 2\alpha(1-N)\right)} \qquad (16)$$

$$N'(r) = 2r\left(\frac{1 - \frac{\Lambda r^2}{3} - N}{r^2 + 2\alpha(1-N)}\right) - \frac{2}{3}\frac{\kappa r^3}{NA^2}\left(\frac{\omega^2\phi^2 + A^2NU(\phi) + N^2A^2\phi'^2}{r^2 + 2\alpha(1-N)}\right) \qquad (17)$$

$$\phi''(r) = -\left(\frac{3}{r} + \frac{A'}{A} + \frac{N'}{N}\right)\phi' - \left(\frac{\omega^2}{N^2A^2} - \frac{1}{2\phi N}\frac{\partial U(\phi)}{\partial \phi}\right)\phi. \qquad (18)$$

Here the prime denotes the derivative with respect to r. These equations possess the following scaling symmetries:

$$
\begin{aligned}
&r \rightarrow \frac{r}{m}, \quad \phi \rightarrow \sigma\phi, \quad \omega \rightarrow m\omega, \\
&\Lambda \rightarrow m^2\Lambda, \quad n \rightarrow n/m^2, \quad \alpha \rightarrow \alpha/\sqrt{m} \qquad (19)
\end{aligned}
$$

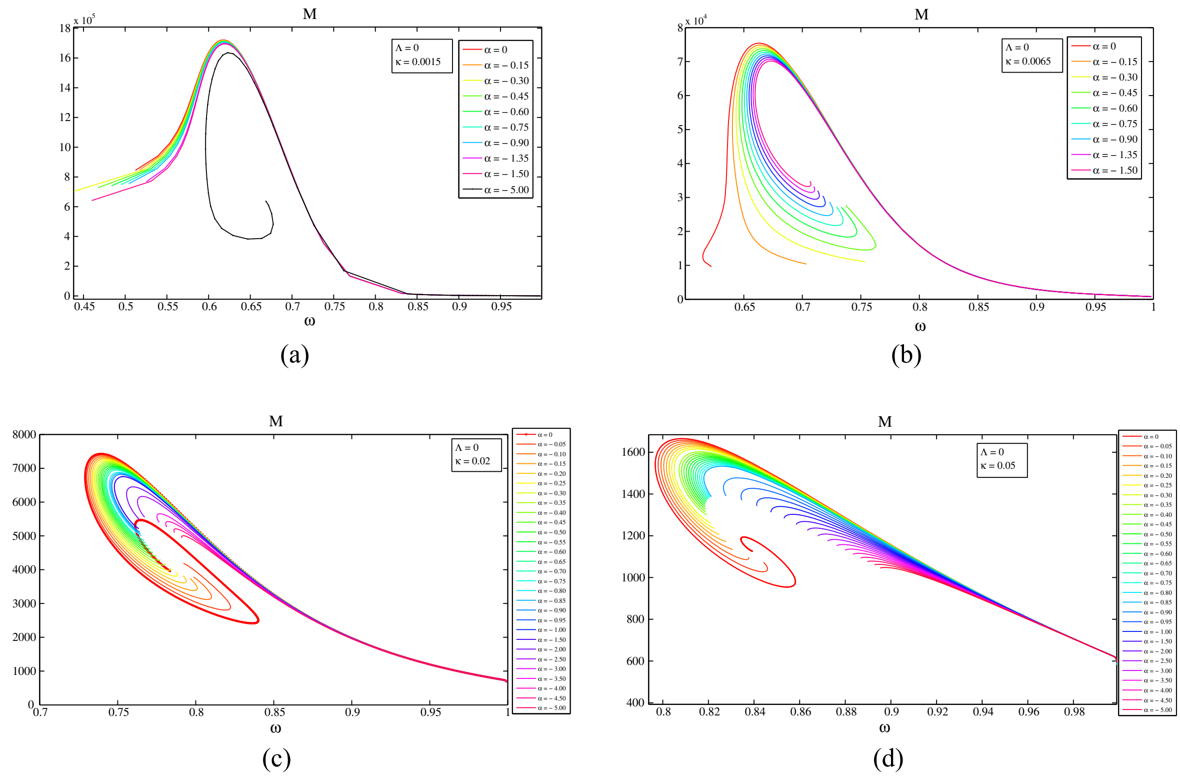

Fig. 1 We give the mass M as function of ω for different values of α: **a** $\kappa = 0.0015$; **b** $\kappa = 0.0065$; **c** $\kappa = 0.02$; **d** $\kappa = 0.05$. Here $\Lambda = 0$

and the equations depend only on the dimensionless coupling constants Λ, α and

$$\kappa = 8\pi G_5 \sigma^2 = 8\pi \frac{\sigma^2}{M_{\rm pl}^2} \tag{20}$$

where $M_{\rm pl}$ is the Planck mass.

To solve these equations, we have to set the appropriate boundary conditions at the origin $r = 0$ and as well as at infinity. At the origin, we require the regularity conditions

$$\phi'(0) = 0, \quad n(0) = 0, \tag{21}$$

and at infinity

$$\phi(\infty) = 0, \quad A(\infty) = 1. \tag{22}$$

Since above system does not have any analytic solution we solve it numerically.

2.2 Definition of mass, charge and radius

As shown before in [1,2,5,27,30,31], we follow [28] and use the same definitions for the radius R, charge Q and mass M as follows:

$$R = \frac{1}{Q}\int \mathrm{d}^4 x r\sqrt{-g}\, j^0 = \frac{2\pi^2}{Q}\int_0^\infty \mathrm{d}r\, r^4 \frac{\omega\phi^2}{AN}, \tag{23}$$

$$Q = \int \mathrm{d}^4 x \sqrt{-g}\, j^0 = 2\pi^2 \int_0^\infty \mathrm{d}r\, r^3 \frac{\omega\phi^2}{AN}. \tag{24}$$

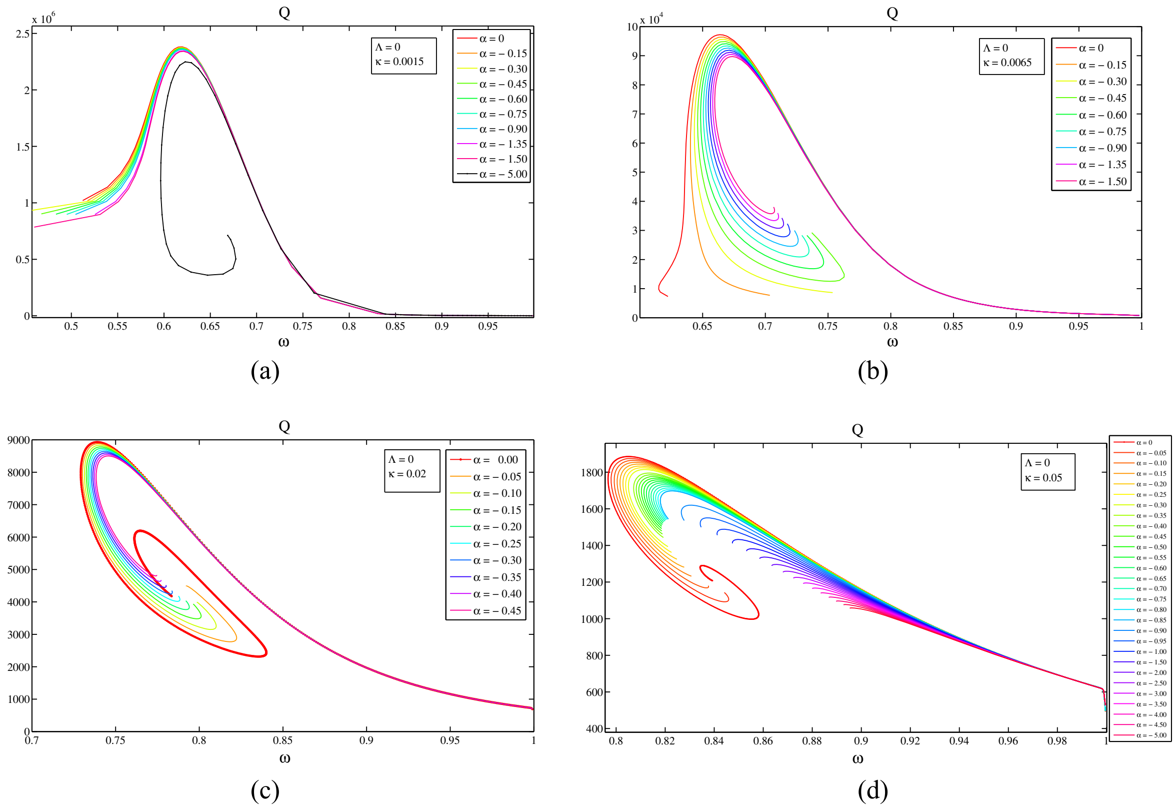

Fig. 2 The charge Q as function of ω for different values of α: **a** $\kappa = 0.0015$; **b** $\kappa = 0.0065$; **c** $\kappa = 0.02$; **d** $\kappa = 0.05$. Here $\Lambda = 0$

Since $A \equiv 1$ and $n \equiv 0$ when $\kappa = 0$, we can use the following definition of mass

$$M = -\int \mathrm{d}^4x\sqrt{-g}T_0^0 = 2\pi^2 \int_0^\infty \mathrm{d}r\, r^3 A \left(N\phi'^2 + \frac{\omega^2\phi^2}{N} + U(\phi)\right), \tag{25}$$

and for $\kappa \neq 0$ case we can use the asymptotic behaviour of the metric function at infinity and the mass can be read off as

$$n(r \gg 1) = M + n_1 r^{-\Delta} + \mathcal{O}(r^{-\Delta}) + \cdots, \tag{26}$$

where $M \simeq n(\infty)$ and n_1 is a constant that depends on AdS radius ℓ.

3 Numerical results

The goal of the paper is to study the basic properties of the boson stars in the presence of negative Gauss–Bonnet coupling in 5-dimensional asymptotically flat and AdS space-time. Let us first start with a flat space-time.

3.1 Flat space-time: $\Lambda = 0$

In Figs. 1, 2, 3 and 4, we plot the mass M, charge Q, the radius R and $\phi(0)$, respectively, as function of ω for different values of Gauss–Bonnet coupling and κ. For small negative values of α, we observe that the behaviour is similar to the standard Einstein gravity case if κ is large. We separate the existence of solutions into three regions. The 1st fundamental branch of solution exists up to ω_{min}. After that point, there is a second branch which exists extending backwards in ω up to a critical value ω_{cr} where a third branch of solutions with

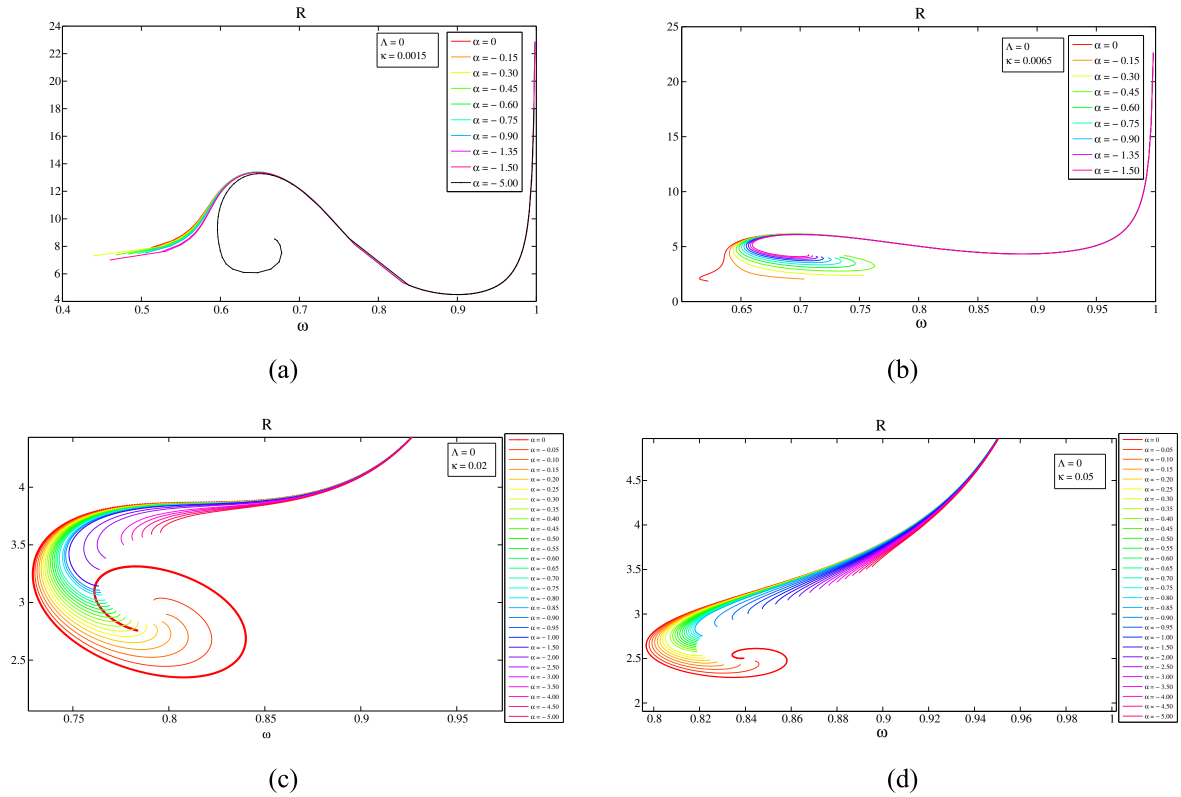

Fig. 3 The radius R as function of ω for different values of α: **a** $\kappa = 0.0015$; **b** $\kappa = 0.0065$; **c** $\kappa = 0.02$; **d** $\kappa = 0.05$. Here $\Lambda = 0$

spiralling behaviour continues. For large negative values of α, this spiralling behaviour disappears. But it is very difficult to find the exact value for α where the 3rd branch disappears. If one compare the 3rd and 2nd branches we can easily see from Figs. 1, 2 and 3 that the mass M, charge Q and radius R always take the higher values on the 3rd branch than the value of 2nd branch at $\omega_{\rm cr}$. The values of the 2nd branch are lower than the values of the 1st branch at $\omega_{\rm min}$. If we continue decreasing α further the 2nd branch also disappears. As a result we end up only with one fundamental branch. In [28], they observed that for large enough positive α the spiral unfolds. We also observed similar effect in Figs. 1a, 2a and 3a for the negative case if the values of κ and α are small enough (say $\kappa = 0.0015$ and $\alpha < -2.0$). If we keep κ fixed and decrease α further we again observe the spiralling behaviour for large negative values of α (see Fig. 5). Similarly, fixing α and increasing κ lead the solutions spiralling (see Figs. 6, 7).

We have also studied the behaviour of the scalar field function at the origin. It is plotted in Fig. 4. In this figure, we give the values of the scalar field function at the origin, $\phi(0)$, as function of ω for different values of α and κ. As shown from Fig. 4, we find that the range of values of $\phi(0)$ is limited and the maximal value for $\phi(0)$ decreases with decreasing α. In the positive α case (see [28]) the $\omega_{\rm min}$ decreases with increasing α and $\omega_{\rm cr}$ takes oscillating behaviour. But in the case when α is negative, the values of $\omega_{\rm min}$ increase with decreasing α and $\omega_{\rm cr}$ first decreases until some critical $\alpha = \alpha_{\rm cr}$ and then it starts to increase further with decreasing α. It is shown more clearly in Fig. 8. At the critical point (the point which two solutions join) numerics become very difficult. In this point, the tip of the metric function $N(r)$ at some $r = r_{\rm cr}$ and as well the central value of the metric function $A(0)$ seems to drop forward to zero. To understand the behaviour of these solutions in more detail we plotted the profiles of metric function in Figs. 9, 10 and 11. Our observations show that the value of metric function $A(r)$ at the origin and the tip of the metric function $N(r)$ decrease with increasing $\phi(0)$ for fixed α and κ. Numerically, it is very difficult to reach $A(0) = 0$ and $N(r_{\rm cr}) = 0$ limit which corresponds to $\phi(0) \to \infty$. It would be interesting to see wether $A(0) \equiv 0$ and $N(r_{\rm cr}) \equiv 0$ at the critical point. Since our numerical code does not converge near $\phi(0) \to \infty$, we could not reach this point.

As we can see from Fig. 12, the minima of the metric function $N(r)$ increases with decreasing α for fixed value of $\phi(0)$. Hence it takes opposite character for the metric function A(r). The value of metric function $A(r)$ at the origin decreases with decreasing α.

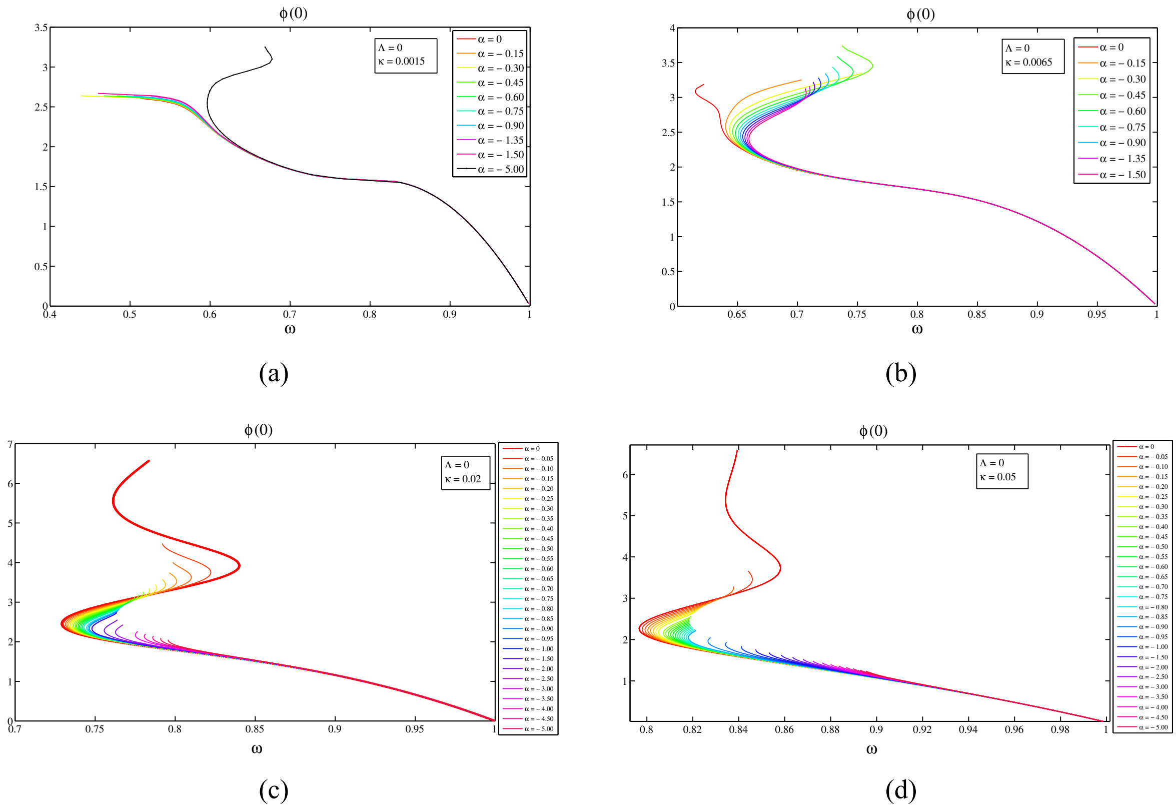

Fig. 4 $\phi(0)$ as function of ω for different values of α: **a** $\kappa = 0.0015$; **b** $\kappa = 0.0065$; **c** $\kappa = 0.02$; **d** $\kappa = 0.05$. Here $\Lambda = 0$

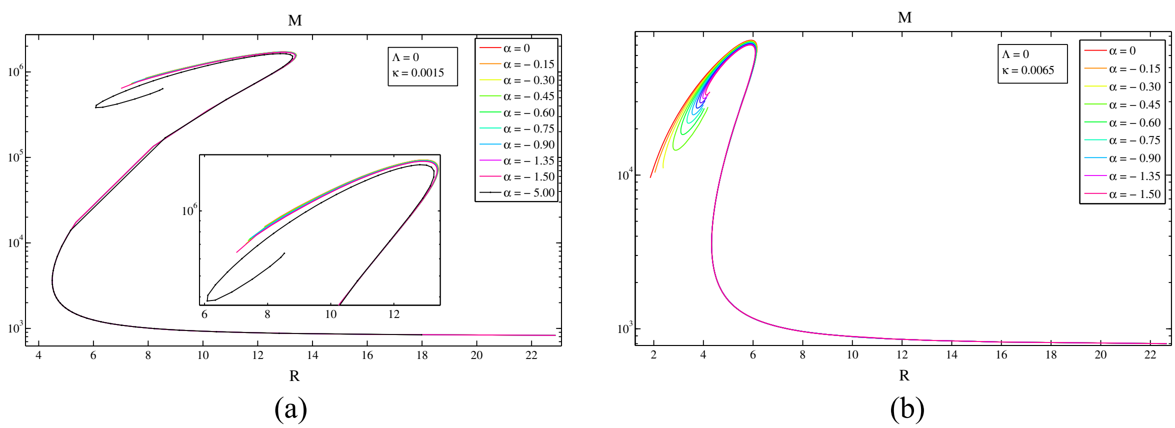

Fig. 5 Mass–radius relation: M as function of R for different values of α: **a** $\kappa = 0.0015$; **b** $\kappa = 0.0065$. Here $\Lambda = 0$

The comparison of the M, Q, R as function of ω, and the mass–radius diagram for $\alpha > 0$ with $\alpha < 0$ case is presented respectively in Figs. 13 and 14. Our analysis show that any changes in α and κ does not affect to maximal frequency and it is always $\omega_{\max} = 1$ for $\Lambda = 0$ case (see Figs. 6 and 13).

3.2 Anti-de Sitter space-time: $\Lambda < 0$

Now let us consider $\Lambda \neq 0$ case. The analysis show that the general pattern of the solutions does not change extremely in this case. As shown in Figs. 15, 16, 17, 18, 19 and 20, the effect of α and κ is same as $\Lambda = 0$ case. As increasing κ and decreasing α, the maximal mass $M_{\max}$, maximal charge $Q_{\max}$ and minimal frequency

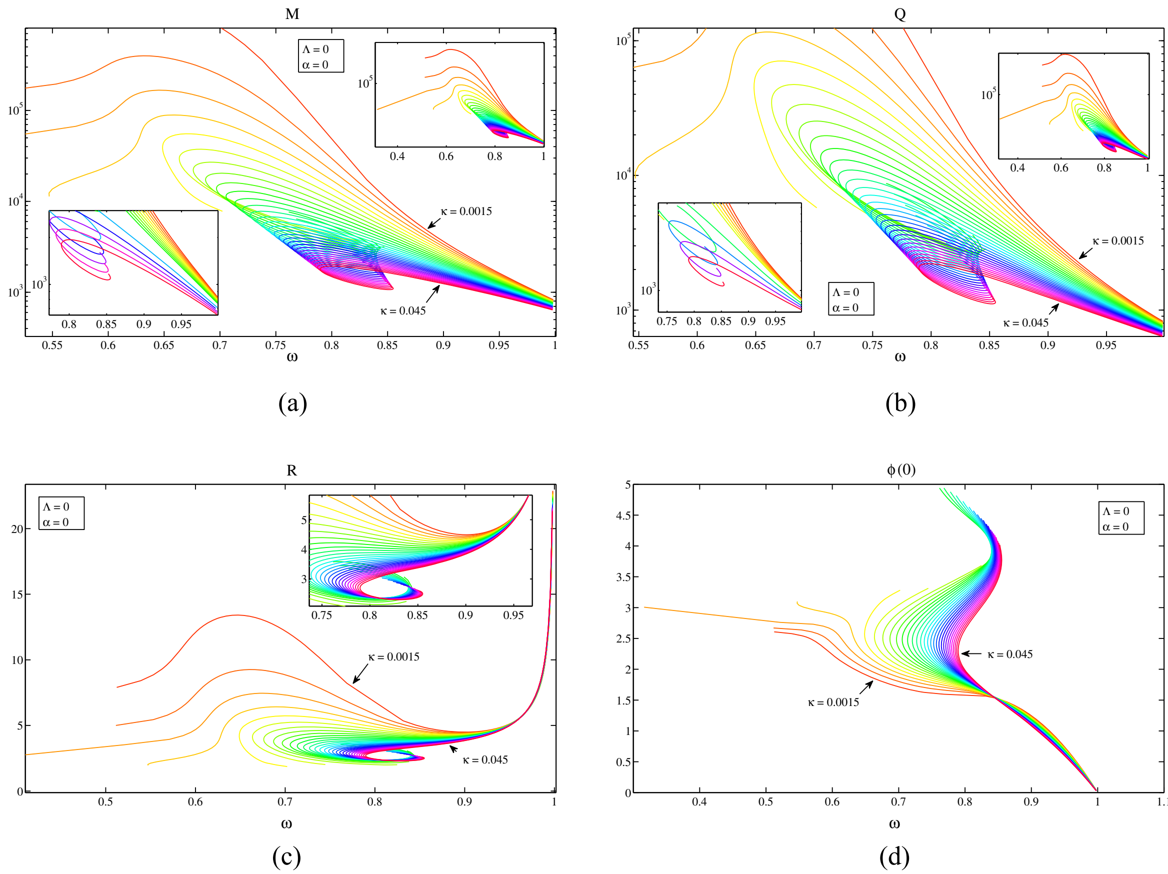

Fig. 6 We show the mass M, charge Q and $\phi(0)$ as function of ω for different values of κ. Here $\alpha = 0$ and $\Lambda = 0$

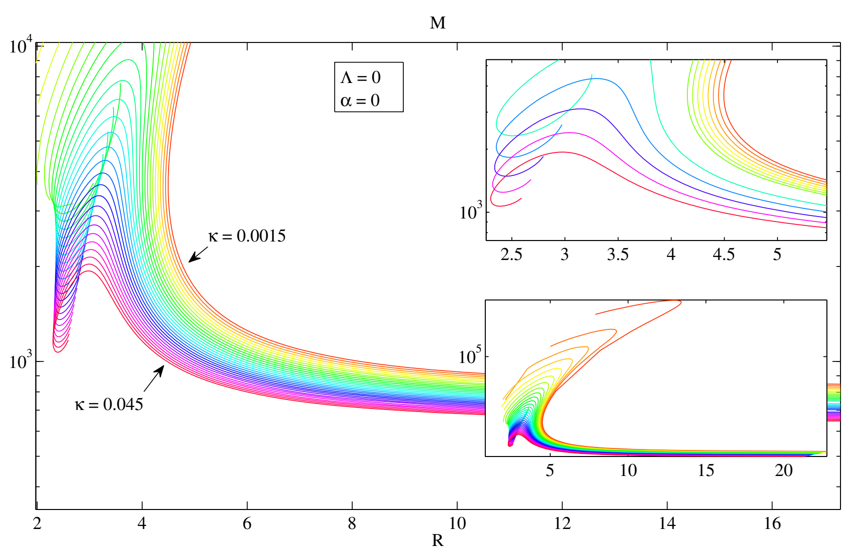

Fig. 7 Mass–radius relation: M as function of R for different values of κ. Here $\alpha = 0$ and $\Lambda = 0$

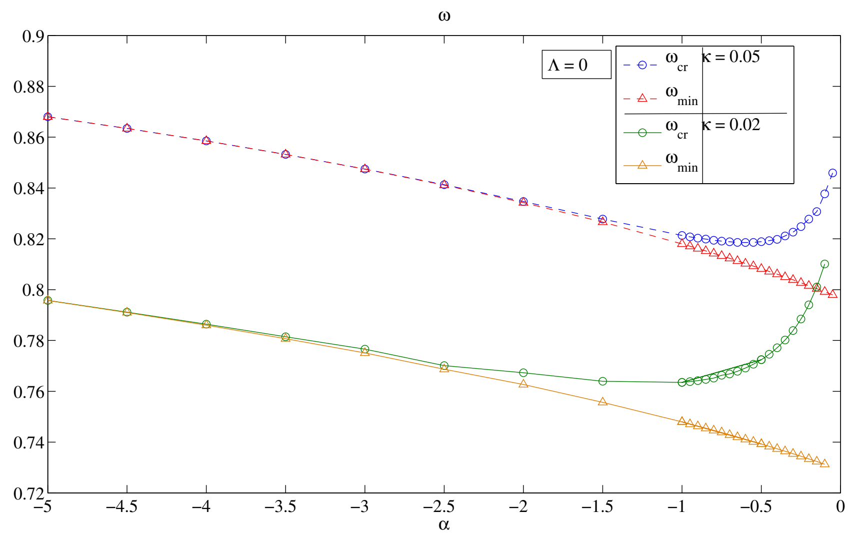

Fig. 8 ω_{min} and ω_{cr} as function of α for two different values of κ. Here $\Lambda = 0$

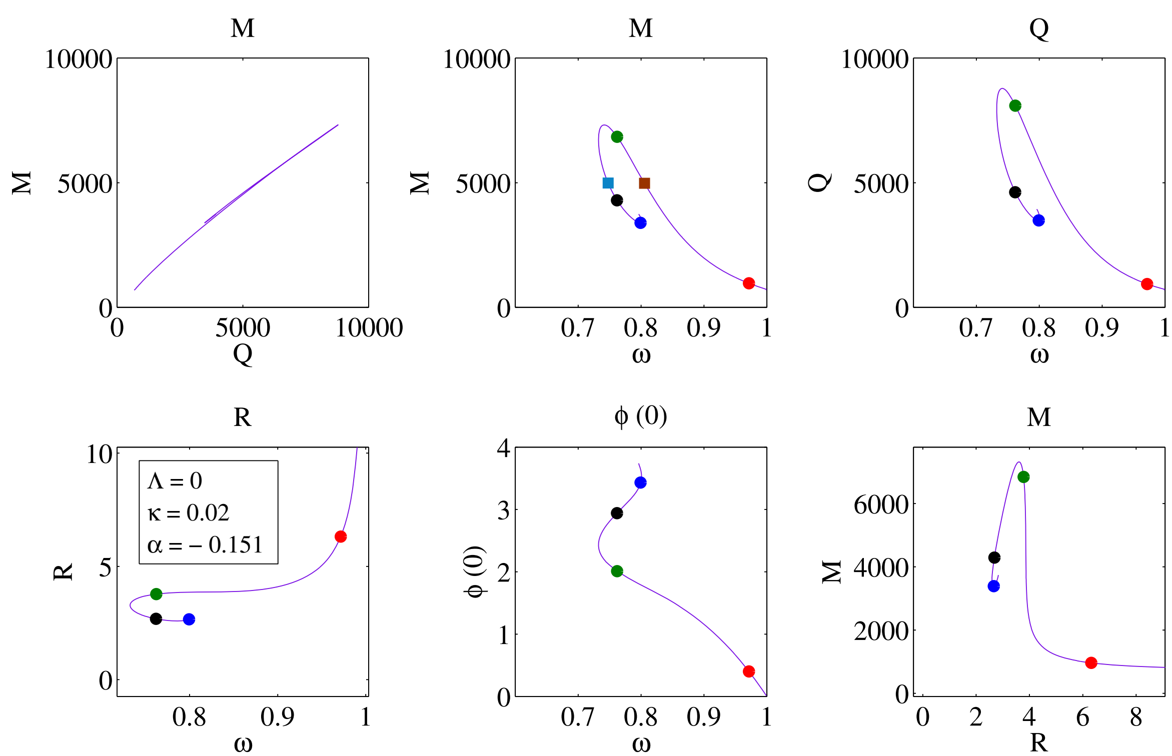

Fig. 9 $M - Q$, $M - \omega$, $Q - \omega$, $R - \omega$, $\phi(0) - \omega$ and $M - R$ plots. Two squares correspond to the solution with equal mass. The circles correspond to the solutions at the different values of $\phi(0)$. Here $\Lambda = 0$

ω_{min} decrease. For small negative values of α, we observe that the behaviour is similar to the flat case if κ is large. Similarly as in the flat case, here we separate the existence of solutions into three regions (see Fig. 21). The 1st fundamental branch of solution exists up to ω_{min}. After that point there is a second branch which exists extending backwards in ω up to a critical value ω_{cr} where a third branch of solutions with spiralling behaviour continues. For large negative values of α this spiralling behaviour disappears. If one compare the 3rd and 2nd branches, we can easily see from Fig. 17 that the mass M, charge Q and radius R always take the higher values on the 3rd branch than the value of 2nd branch at ω_{cr} when κ is large. But when κ is small enough we observe

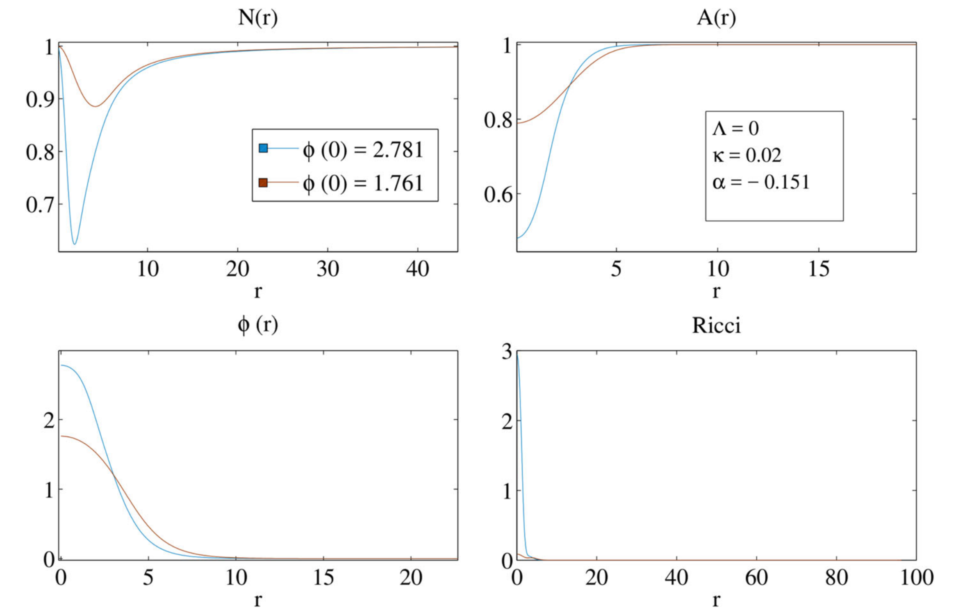

Fig. 10 The profiles of functions with equal mass as indicated with squares in Fig. 9. Here $\Lambda = 0$

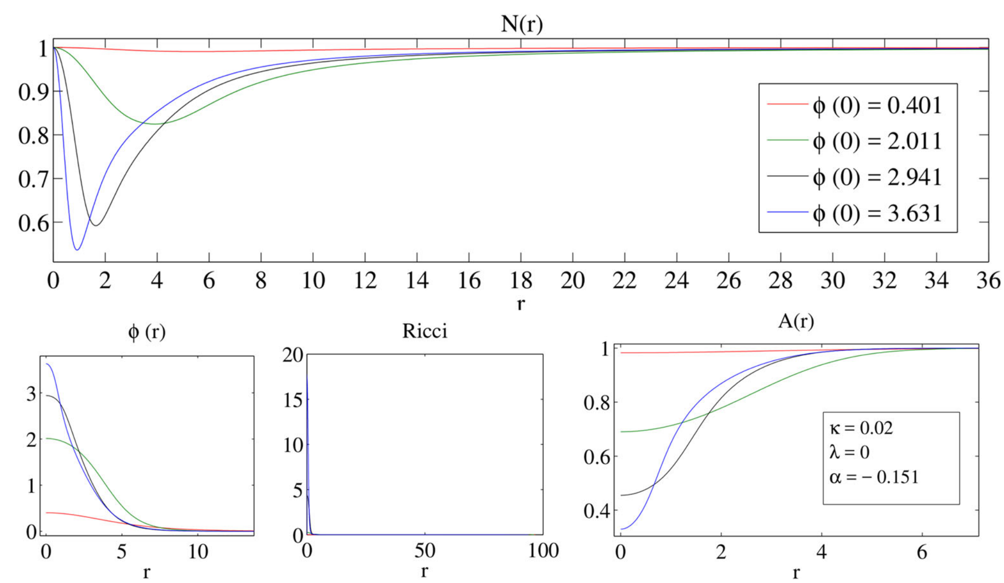

Fig. 11 Profiles of functions at the different values of $\phi(0)$ as indicated with circles in Fig. 9. Here $\Lambda = 0$

the opposite, the values of the 3nd branch are lower than the values of the 2nd branch at ω_{cr}. If we continue decreasing α further, 2nd branch also disappears. As a result we end up only with one fundamental branch. Similarly, as in the flat case, when α is negative, the values of $\omega_{\min}$ increase with decreasing α and ω_{cr} first decreases until some critical $\alpha = \alpha_{\text{cr}}$ and then it starts to increase further with decreasing α. It is shown more clearly in Fig. 22 for $\Lambda = -0.02$ and $\kappa = 0.01$.

Next we discuss the properties of solutions for different values of cosmological constant Λ for fixed Gauss–Bonnet coupling α and the gravitational constant κ. If one compare the maximal mass of boson stars for $\Lambda < 0$ with $\Lambda = 0$ case (see Figs. 23, 24), it is shown clearly from the figures that in the flat case it is always higher than AdS case. The same feature occurs for maximal charge $Q_{\max}$ and maximal radius $R_{\max}$. In the flat case, the maximal charge and the maximal radius is always bigger than the case in AdS.

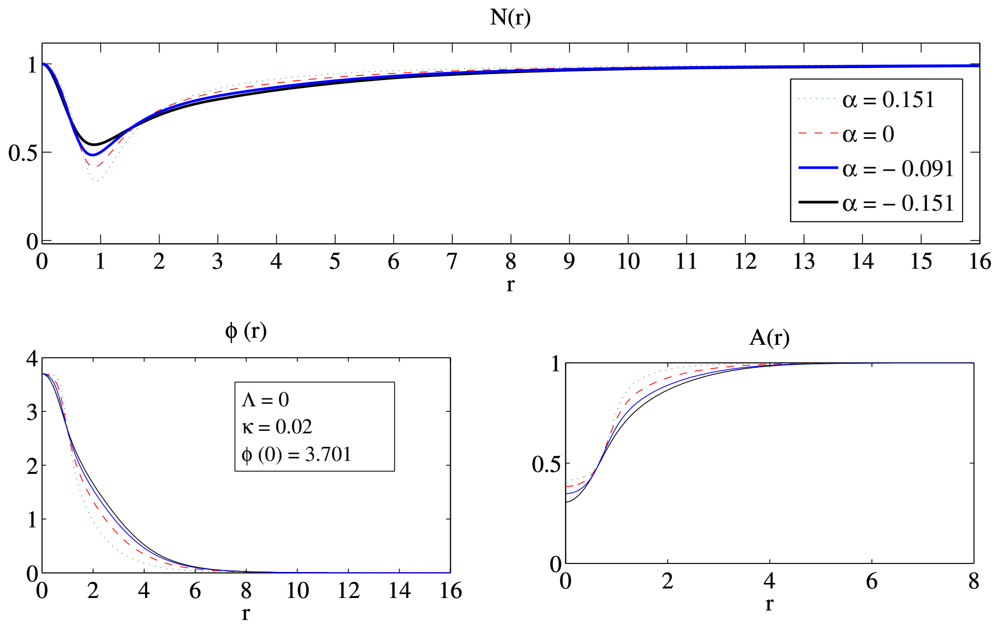

Fig. 12 Comparing the profiles of functions for the different values of α. Here $\phi(0) = 3.701$, $\kappa = 0.02$ and $\Lambda = 0$

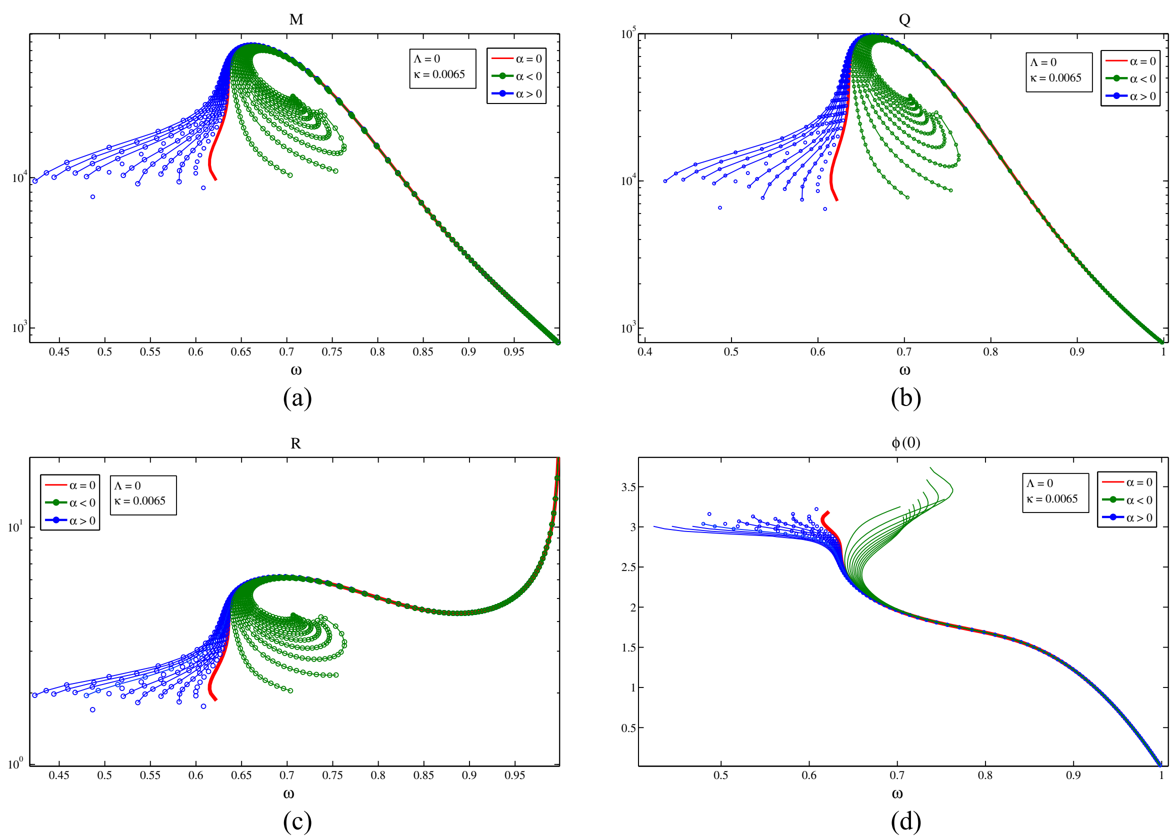

Fig. 13 The comparison of the mass M, charge Q, radius R and $\phi(0)$ for different values of α. The red curve corresponds to the $\alpha = 0$ case while the blue and green lines correspond to $\alpha > 0$ and $\alpha < 0$ case, respectively. Here $\kappa = 0.0065$ and $\Lambda = 0$

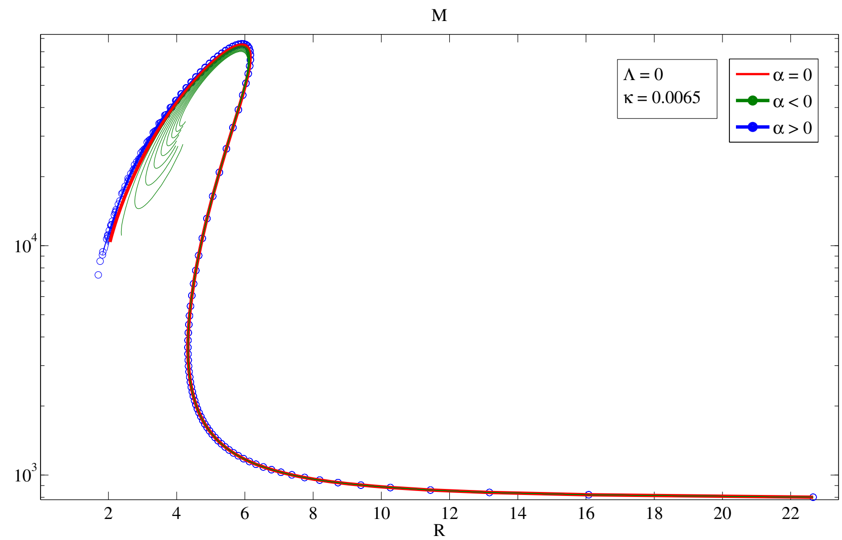

Fig. 14 Mass–radius relation: M as function of R for different values of α. The red curve corresponds to the $\alpha = 0$ case while the blue and green lines correspond to $\alpha > 0$ and $\alpha < 0$ case, respectively. Here $\kappa = 0.0065$ and $\Lambda = 0$

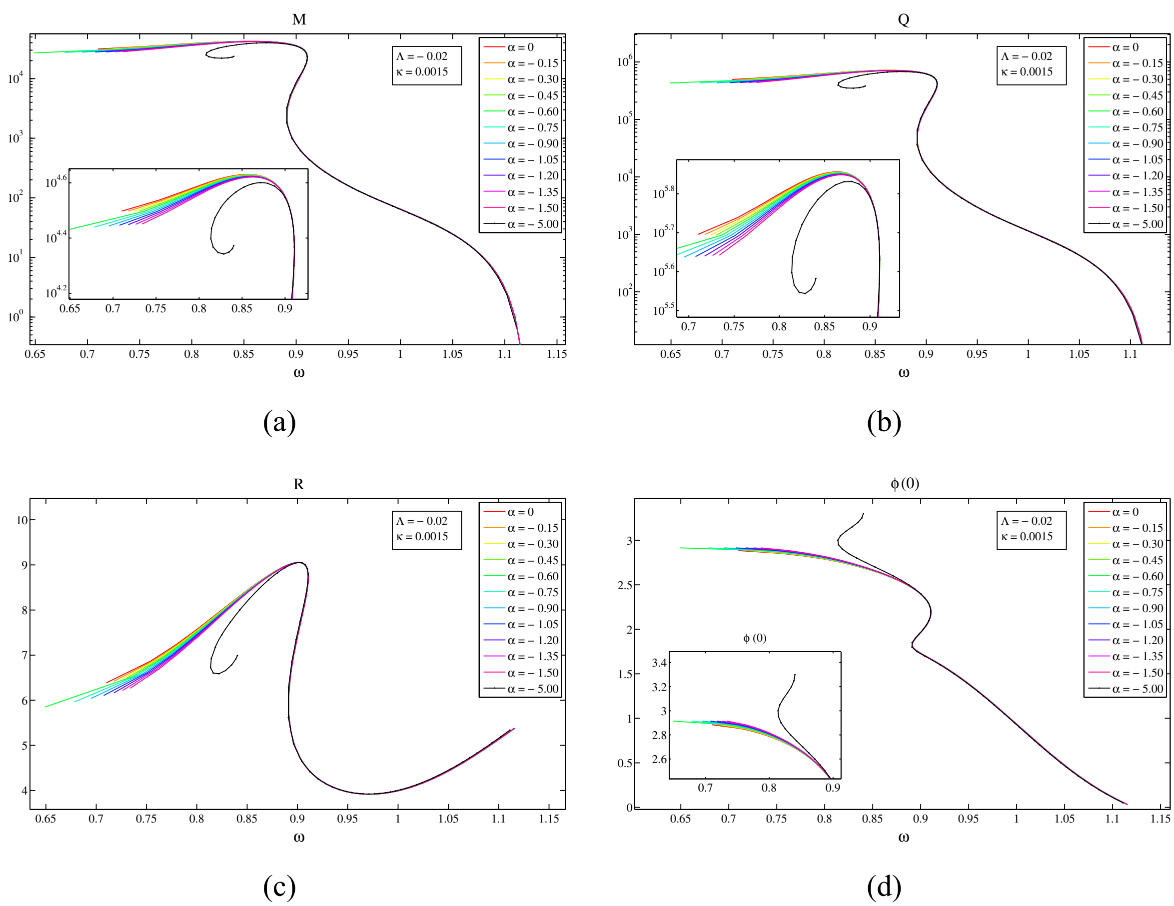

Fig. 15 We give the mass M, the charge Q, $\phi(0)$ as function of ω for different values of α. Here $\kappa = 0.0015$ and $\Lambda = -0.02$

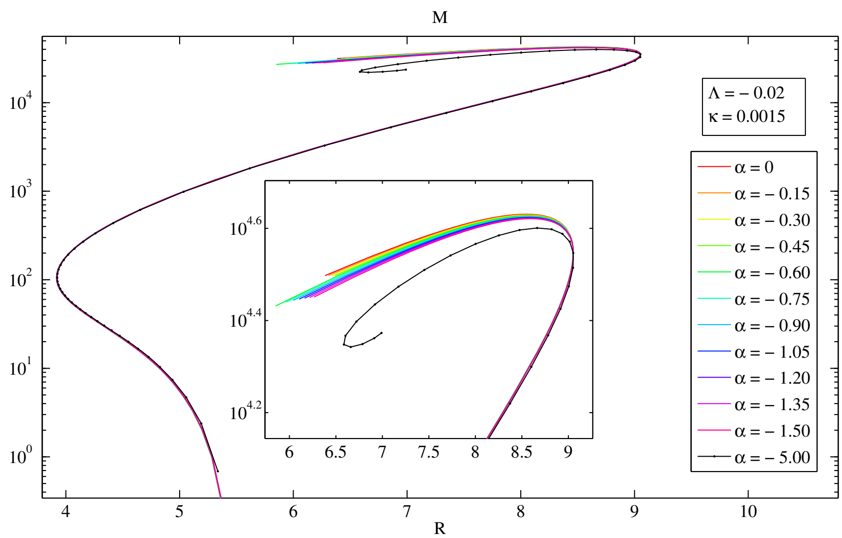

Fig. 16 Mass–radius relation: M as function of R for different values of α. Here $\kappa = 0.0015$ and $\Lambda = -0.02$

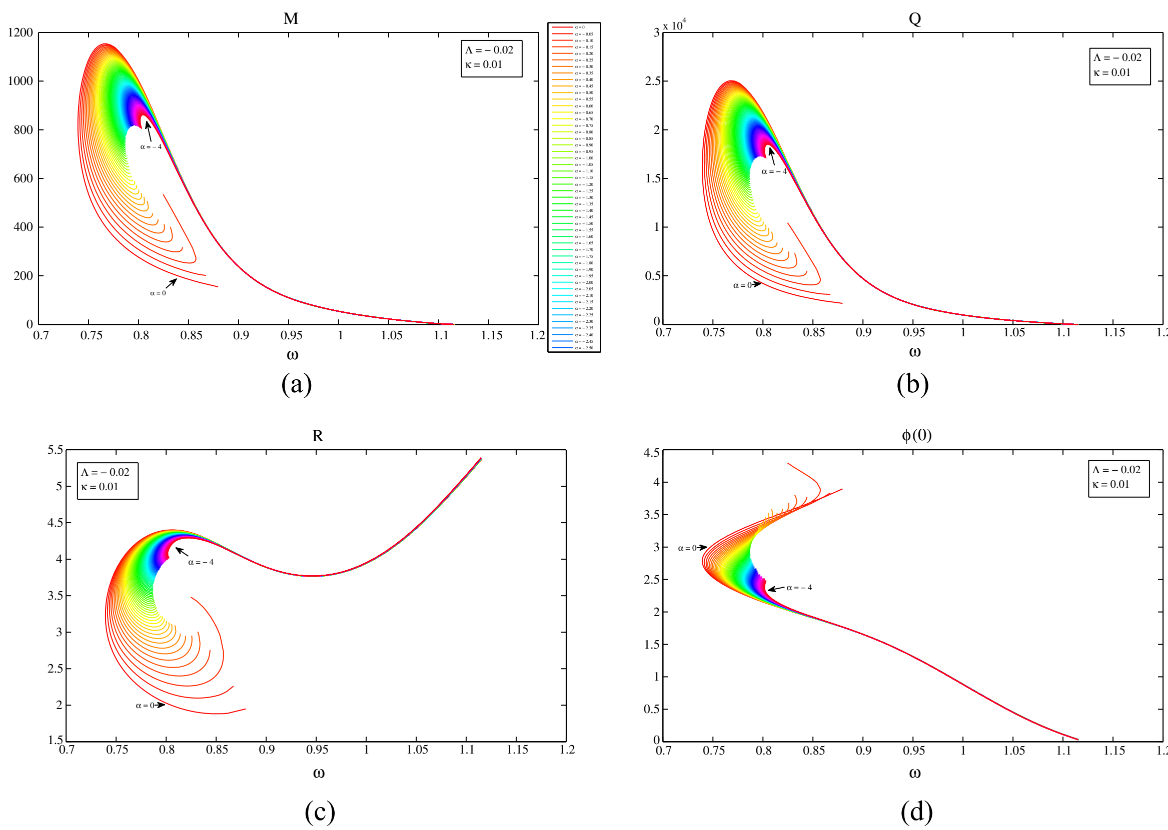

Fig. 17 We give the mass M, the charge Q, $\phi(0)$ as function of ω for different values of α. Here $\kappa = 0.01$ and $\Lambda = -0.02$

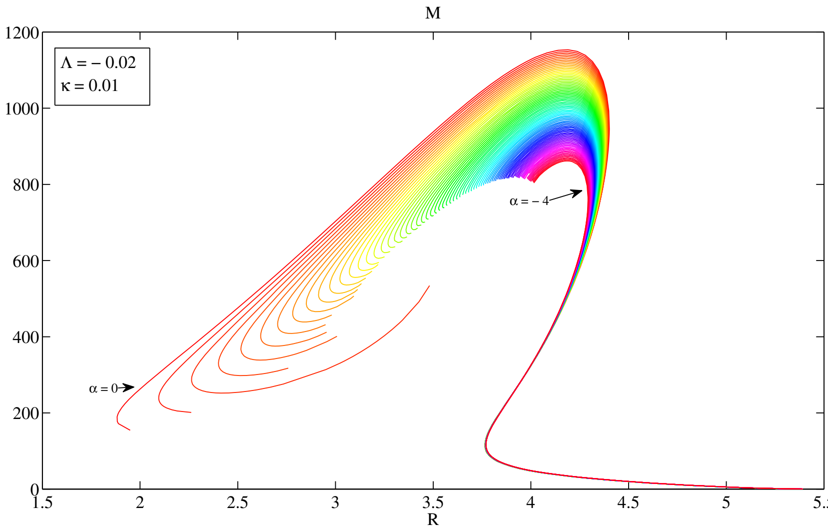

Fig. 18 Mass–radius relation: M as function of R for different values of α. Here $\kappa = 0.01$ and $\Lambda = -0.02$

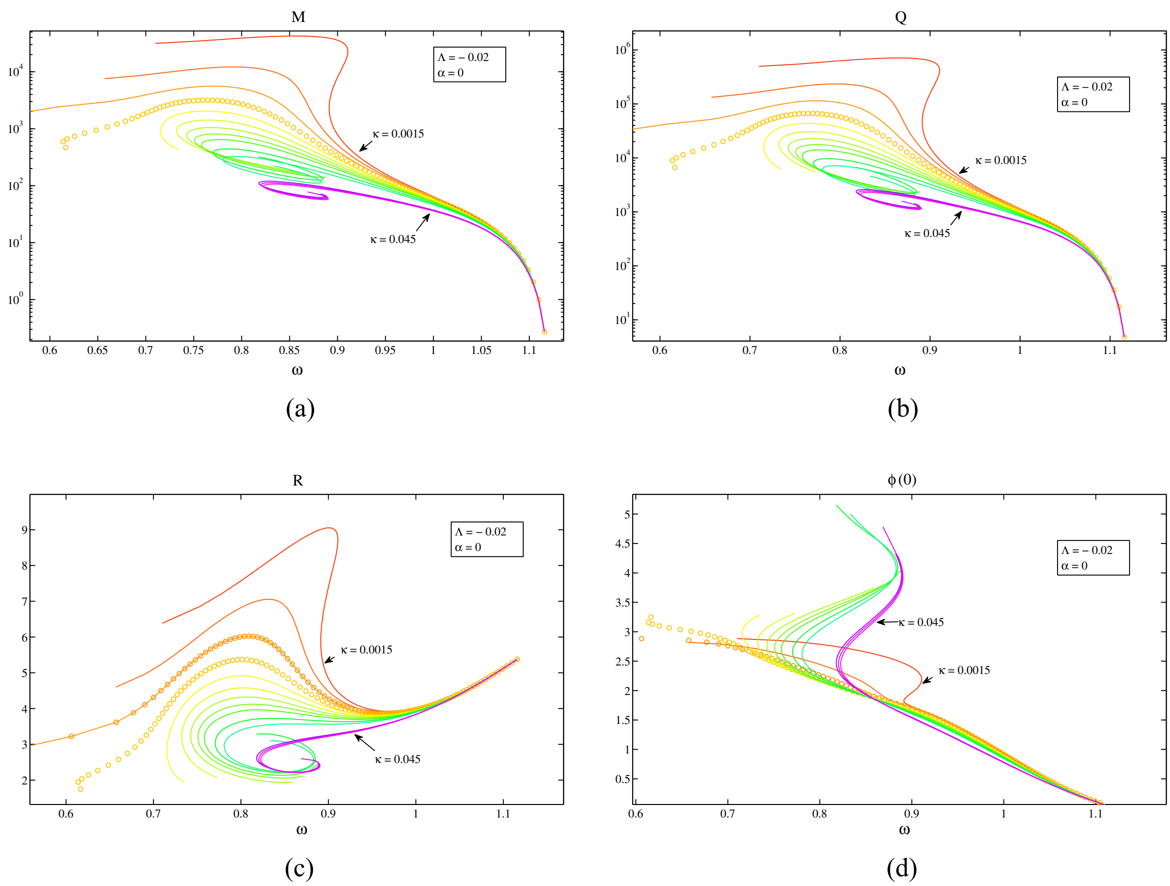

Fig. 19 We give the mass M, the charge Q, $\phi(0)$ as function of ω for different values of κ. Here $\alpha = 0$ and $\Lambda = -0.02$

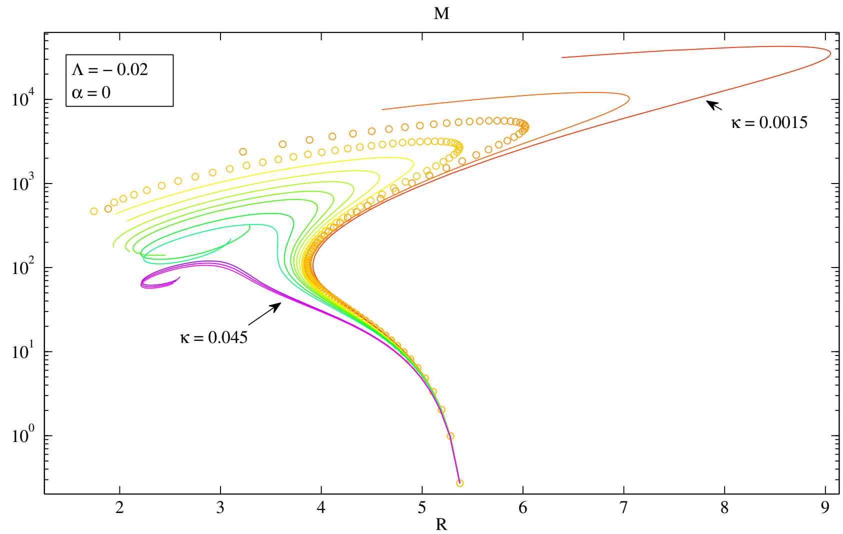

Fig. 20 Mass–radius relation: M as function of R for different values of κ. Here $\alpha = 0$ and $\Lambda = -0.02$

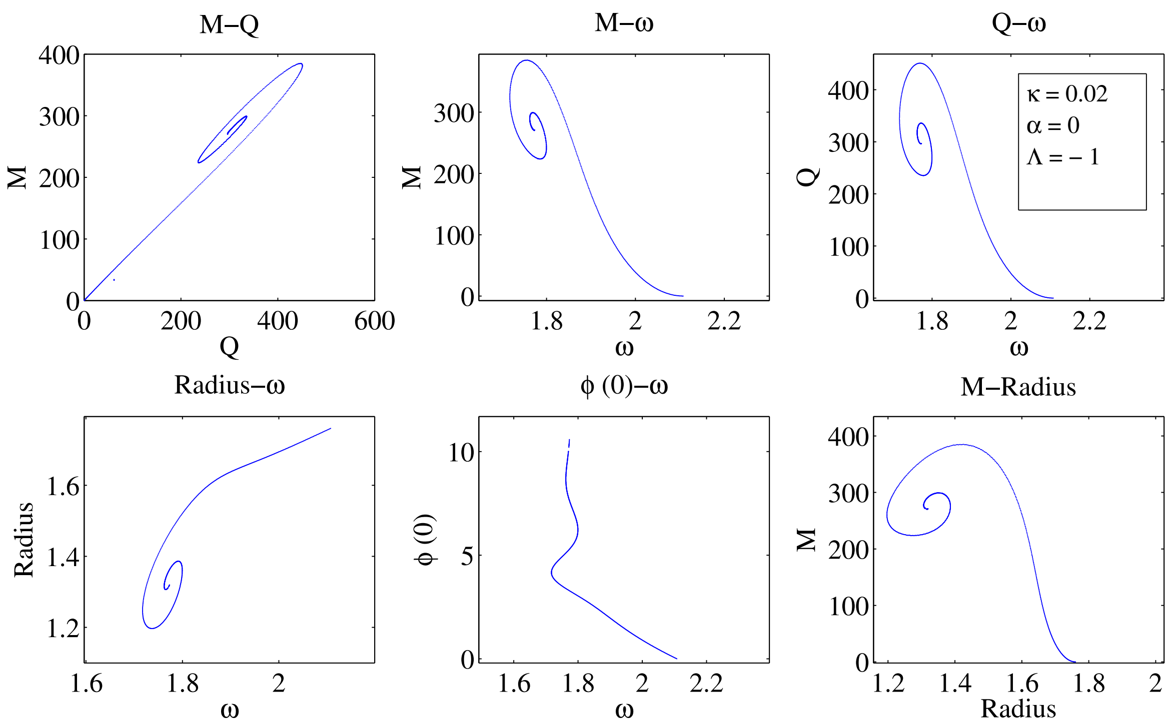

Fig. 21 $M - Q$, $M - \omega$, $Q - \omega$, $R - \omega$, $\phi(0) - \omega$ and $M - R$ plots. Here $\alpha = 0$, $\kappa = 0.02$ and $\Lambda = -1$

Comparing the flat case with the AdS space time the small decrease of Λ lowers the maximal mass $M_{\max}$ suddenly. These can be seen in Fig. 23a. But with decreasing Λ, the maximal frequency $\omega_{\max}$ increases being $\omega_{\max} > 1$.

4 Conclusion

In this paper, we have studied the properties of asymptotically flat and anti-de Sitter boson stars in five-dimensional Gauss–Bonnet gravity in more detail for different values of the cosmological constant Λ, Gauss–Bonnet coupling α and the gravitational constant κ. First, we studied the flat case. In [28], the authors showed

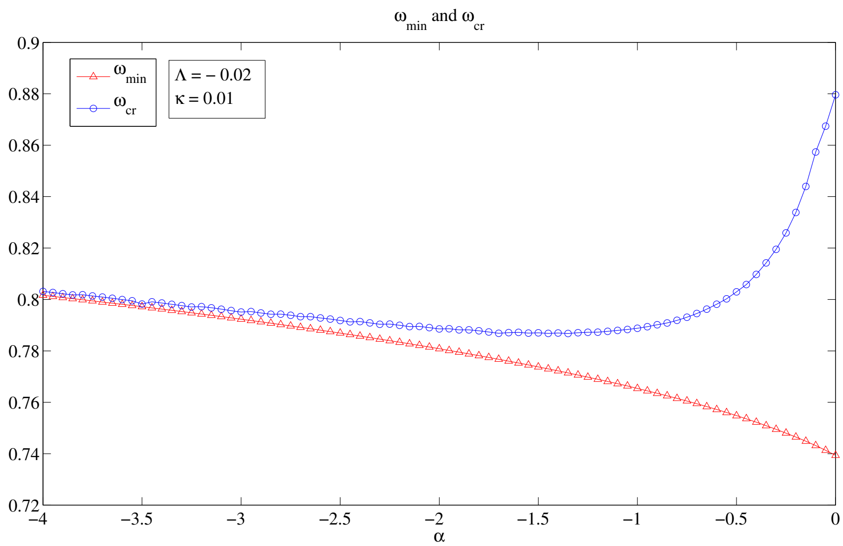

Fig. 22 ω_{min} and ω_{cr} as function of α for $\kappa = 0.01$ and $\Lambda = -0.02$

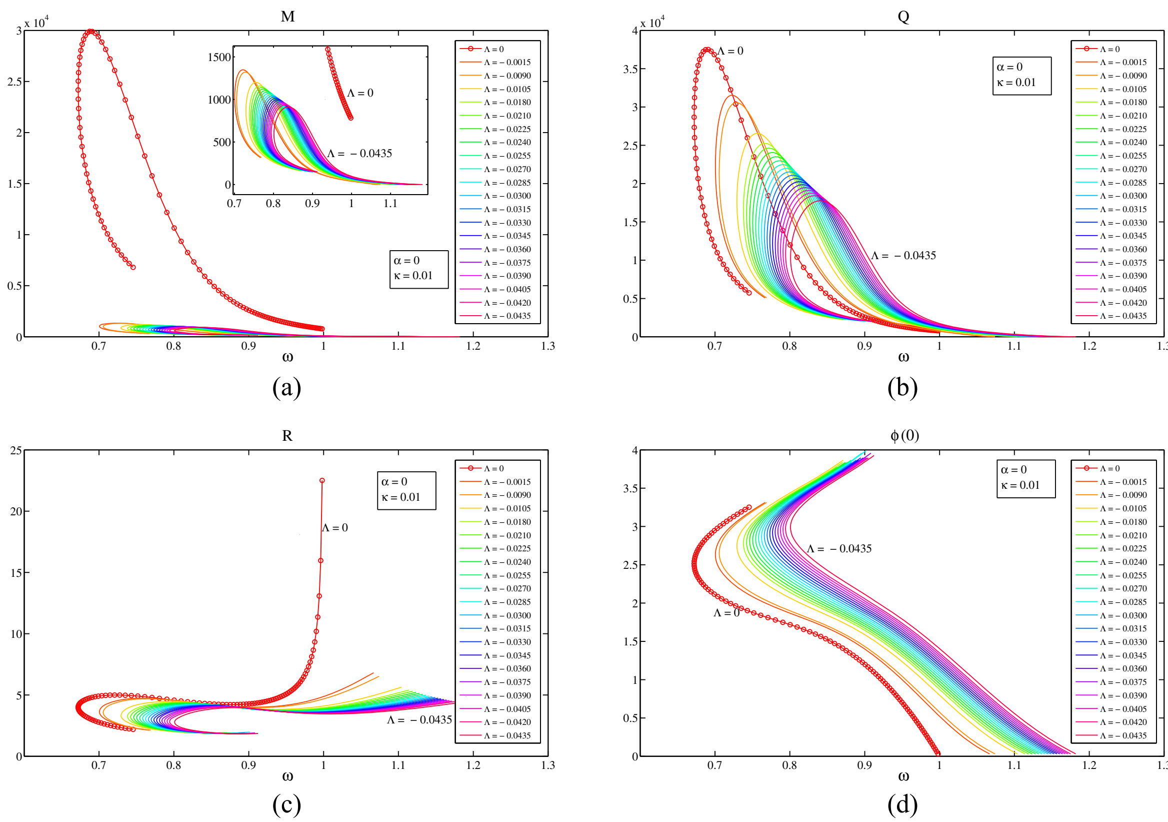

Fig. 23 The comparison of the mass M, charge Q, radius R and $\phi(0)$ for different values of Λ. Here $\alpha = 0$ and $\kappa = 0.01$

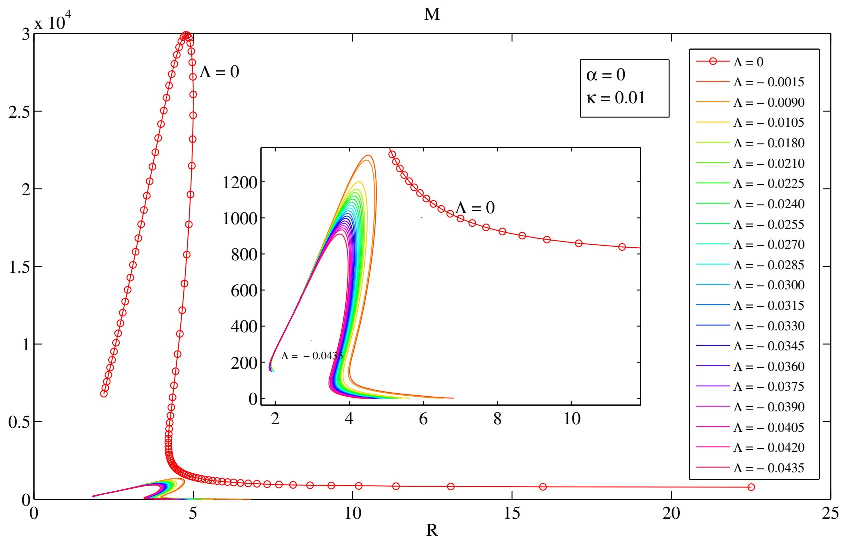

Fig. 24 Mass–radius relation: M as function of R for different values of Λ. Here $\alpha = 0$ and $\kappa = 0.01$

that the spiralling behaviour characteristic for boson stars is observed for $\alpha = 0$. But our analysis show that this is valid only if κ is large enough. We find that the spiralling behaviour disappears for small enough κ even when $\alpha = 0$. We also observed that the maximal mass M, the maximal charge Q and the maximal frequency is always larger in excited solutions than the ground solutions. Comparing the flat case with the AdS space time the small decrease of Λ lowers the maximal mass $M_{\max}$, maximal charge $Q_{\max}$ and minimal frequency $\omega_{\min}$. On the basis of our numerical analysis, we can state:

- the maximal mass $M_{\max}$, the maximal charge $Q_{\max}$, the maximal radius $R_{\max}$ and the minimal radius $R_{\min}$ of the boson star decreases with decreasing cosmological constant Λ;
- the minimal and the maximal internal frequency increases with decreasing cosmological constant Λ;
- the $\omega_{\min}$ increases with decreasing Gauss–Bonnet coupling α in both flat and AdS space-time;
- the ω_{cr} decreases with decreasing Gauss–Bonnet coupling α in both flat and AdS space-time;
- the $\omega_{\min}$ and ω_{cr} increases with increasing gravitation constant κ;
- the maximal mass $M_{\max}$, the maximal charge $Q_{\max}$, the maximal radius $R_{\max}$ and the minimal radius $R_{\min}$ decreases with increasing κ in both flat and AdS space-time.

It has been previously shown [25] that the boson star solutions exist only in a limited parameter range of ω. This parameter range depends on the choice of potential and the cosmological constant Λ. In a flat space-time for our potential (5) it obeys $\omega \in [0 : 1]$. However, we observed that the maximal frequency increases with decreasing Λ and it is always bigger than one ($\omega_{\max} > 1$) in the AdS space-time. We find that changing the Gauss–Bonnet coupling α or the gravitational constant κ does not make any influence on the maximal frequency $\omega_{\max}$ in both flat and AdS space-time.

Acknowledgements Author gratefully acknowledges support within the framework of the DFG Research Training Group 1620 "*Models of gravity*". Author would like to thank Betti Hartmann and Jürgen Riedel for their help in the early stage of the work. This research is supported by Grant F3-2020092957 of the Uzbekistan Ministry for Innovative Development.

Funding The authors have not disclosed any funding.

Declarations

Conflict of interest The authors have not disclosed any competing interests.

References

1. Arodź, H.; Lis, J.: Compact Q-balls in the complex signum-Gordon model. Phys. Rev. D **77**(10), 107702 (2008)
2. Arodź, H.; Lis, J.: Compact Q-balls and Q-shells in a scalar electrodynamics. Phys. Rev. D **79**(4), 045002 (2009)
3. Ascher, U.; Christiansen, J.; Russell, R.D.: A collocation solver for mixed order systems of boundary value problems. Math. Comput. **33**(146), 659–679 (1979)
4. Ascher, U.; Christiansen, J.; Russell, R.D.: Collocation software for boundary-value odes. ACM Trans. Math. Softw. **7**(2), 209–222 (1981)
5. Astefanesei, D.; Radu, E.: Boson stars with negative cosmological constant. Nucl. Phys. B **665**, 594–622 (2003)
6. ATLAS Collaboration: Observation of a new particle in the search for the standard model Higgs boson with the ATLAS detector at the LHC. Phys. Lett. B **716**(1), 1–29 (2012)
7. Barclay, L.; Gregory, R.; Kanno, S.; Sutcliffe, P.: Gauss–Bonnet holographic superconductors. J. High Energy Phys. **2010**, 29 (2010)
8. Brihaye, Y.; Hartmann, B.: Holographic superconductors in $3+1$ dimensions away from the probe limit. Phys. Rev. D **81**(12), 126008 (2010)
9. Brihaye, Y.; Hartmann, B.: Stability of Gauss–Bonnet black holes in anti-de Sitter space-time against scalar field condensation. Phys. Rev. D **84**(8), 084008 (2011)
10. Brihaye, Y.; Hartmann, B.: Hairy charged Gauss–Bonnet solitons and black holes. Phys. Rev. D **85**(12), 124024 (2012)
11. Brihaye, Y.; Hartmann, B.: A scalar field instability of rotating and charged black holes in $(4+1)$-dimensional anti-de Sitter space-time. J. High Energy Phys. **2012**, 50 (2012)
12. Brihaye, Y.; Radu, E.: Black objects in the Einstein–Gauss–Bonnet theory with negative cosmological constant and the boundary counterterm method. J. High Energy Phys. **2008**(9), 006 (2008)
13. Brihaye, Y.; Riedel, J.: Rotating boson stars in five-dimensional Einstein–Gauss–Bonnet gravity. Phys. Rev. D **89**(10), 104060 (2014)
14. Brihaye, Y.; Hartmann, B.; Tojiev, S.: Formation of scalar hair on Gauss–Bonnet solitons and black holes. Phys. Rev. D **87**(2), 024040 (2013)
15. Brihaye, Y.; Hartmann, B.; Tojiev, S.: AdS solitons with conformal scalar hair. Phys. Rev. D **88**(10), 104006 (2013)
16. Brihaye, Y.; Hartmann, B.; Tojiev, S.: Stability of charged solitons and formation of boson stars in five-dimensional anti-de Sitter spacetime. Class. Quantum Gravity **30**(11), 115009 (2013)
17. Brihaye, Y.; Diemer, V.; Hartmann, B.: Charged Q-balls and boson stars and dynamics of charged test particles. Phys. Rev. D **89**(8), 084048 (2014)
18. Brihaye, Y.; Hartmann, B.; Riedel, J.: Self-interacting boson stars with a single Killing vector field in anti-de Sitter space-time. Phys. Rev. D **92**(4), 044049 (2015)
19. Brihaye, Y.; Cisterna, A.; Hartmann, B.; Luchini, G.: From topological to nontopological solitons: kinks, domain walls, and Q-balls in a scalar field model with a nontrivial vacuum manifold. Phys. Rev. D **92**(12), 124061 (2015)
20. Copeland, E.J.; Tsumagari, M.I.: Q-balls in flat potentials. Phys. Rev. D **80**(2), 025016 (2009)
21. Dias, Ó.J.C.; Monteiro, R.; Reall, H.S.; Santos, J.E.: A scalar field condensation instability of rotating anti-de Sitter black holes. J. High Energy Phys. **2010**, 36 (2010)
22. Dias, Ó.J.C.; Figueras, P.; Minwalla, S.; Mitra, P.; Monteiro, R.; Santos, J.E.: Hairy black holes and solitons in global AdS_5. J. High Energy Phys. **2012**, 117 (2012)
23. Dine, M.; Kusenko, A.: Origin of the matter–antimatter asymmetry. Rev. Mod. Phys. **76**, 1–30 (2003)
24. Gentle, S.A.; Rangamani, M.; Withers, B.: A soliton menagerie in AdS. J. High Energy Phys. **2012**, 106 (2012)
25. Hartmann, B.; Riedel, J.: Glueball condensates as holographic duals of supersymmetric Q-balls and boson stars. Phys. Rev. D **86**(10), 104008 (2012)
26. Hartmann, B.; Riedel, J.: Supersymmetric Q-balls and boson stars in $(d+1)$ dimensions. Phys. Rev. D **87**(4), 044003 (2013)
27. Hartmann, B.; Kleihaus, B.; Kunz, J.; Schaffer, I.: Compact boson stars. Phys. Lett. B **714**(1), 120–126 (2012)
28. Hartmann, B.; Riedel, J.; Suciu, R.: Gauss–Bonnet boson stars. Phys. Lett. B **726**(4–5), 906–912 (2013)
29. Hartmann, B.; Kleihaus, B.; Kunz, J.; Schaffer, I.: Compact (A)dS boson stars and shells. Phys. Rev. D **88**(12), 124033 (2013)
30. Kleihaus, B.; Kunz, J.; Lämmerzahl, C.; List, M.: Charged boson stars and black holes. Phys. Lett. B **675**(1), 102–109 (2009)
31. Kleihaus, B.; Kunz, J.; Lämmerzahl, C.; List, M.: Boson shells harboring charged black holes. Phys. Rev. D **82**(10), 104050 (2010)
32. Kusenko, A.; Shaposhnikov, M.: Supersymmetric Q-balls as dark matter. Phys. Lett. B **418**(1), 46–54 (1998)
33. Kusenko, A.; Kuzmin, V.; Shaposhnikov, M.; Tinyakov, P.G.: Experimental signatures of supersymmetric dark-matter Q-balls. Phys. Rev. Lett. **80**, 3185–3188 (1998)
34. Schunck, F.E.; Liddle, A.R.: Boson stars in the centre of galaxies? In: Hehl, F.W., Kiefer, C., Metzler, R.J.K. (eds.) Black Holes: Theory and Observation, pp. 285–288. Springer, Berlin (1998)